

NATIONAL AERONAUTICAL
ESTABLISHMENT

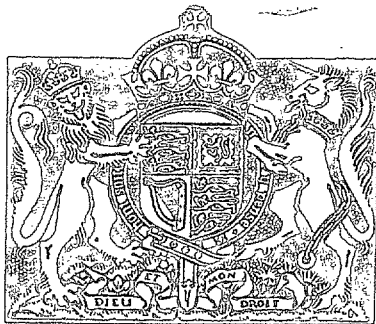
19 OCT 1951

NR. CLAPHAM, BEDS.

NATIONAL AERONAUTICAL ESTABLISHMENT
LIBRARY

N. A. E. Library

R. & M. No. 2618
(5941)
A.E.C. Technical Report



MINISTRY OF SUPPLY

AERONAUTICAL RESEARCH COUNCIL
REPORTS AND MEMORANDA

Stress Diffusion Adjacent to Gaps in the Inter-spar Skin of a Stressed-skin Wing

By

M. FINE, B.A. and H. G. HOPKINS, M.Sc.

Crown Copyright Reserved

LONDON: HIS MAJESTY'S STATIONERY OFFICE

1951

PRICE 3s 6d NET

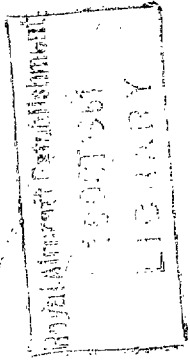
Stress Diffusion Adjacent to Gaps in the Inter-spar Skin of a Stressed-skin Wing

By

M. FINE, B.A. and H. G. HOPKINS, M.Sc.

COMMUNICATED BY THE PRINCIPAL DIRECTOR OF SCIENTIFIC RESEARCH (AIR),
MINISTRY OF SUPPLY

*Reports and Memoranda No. 2618**
May, 1942



Summary.—The diffusion of stress in the neighbourhood of chordwise gaps in the wing surface is an important structural design problem. Such gaps occur at wing joints and at undercarriage and bomb-bay cut-outs, and can involve local stress concentrations which require to be estimated. This report gives, subject to certain simplifications (including representation of the stringers by an equivalent sheet, carrying direct end load only), a theoretical analysis of the problem, and derives formulae for the stress distribution. Approximate formulae are found for (i) the direct stress in the flanges and (ii) the shear stress in the skin at the flanges and at the chordwise gap. These approximate formulae, applicable with negligible error when chordwise gaps are not closer than about one and a half times the inter-spar distance, enable a rapid estimate to be made of the stress concentration. A numerical example to illustrate the application to design is given, and shows that the maximum additional skin shear stress can be as much as two to three times the maximum additional flange direct stress. Although various factors (for example, flexibility of riveted joints between the spar flanges and the skin, local buckling and plastic flow) are likely to reduce the stress concentration if present calculations predict it to be high, some reinforcement of the skin is likely to be necessary.

1. *Introduction.*—The diffusion of stress in the neighbourhood of chordwise gaps in the wing surface is an important structural design problem. Such gaps occur at wing joints and at undercarriage and bomb-bay cut-outs, and can involve local stress concentrations which require to be estimated. This report gives, subject to certain simplifications, described and discussed in section 2, a theoretical analysis of the problem, the mathematical details of which are set out in the Appendix. The notation is given in section 3. Approximate formulae are given for (i) the direct stress in the flanges (section 4.1) and (ii) the shear stress in the skin at the flanges (section 4.2) and at the chordwise gap (section 4.3). These approximate formulae, applicable with negligible error when chordwise gaps are not closer than about one and a half times the inter-spar distance, enable a rapid estimate to be made of the stress concentration. A numerical example to illustrate application to design is given in section 5. The conclusions of the investigation are given in section 6.

2. *Statement of Problem and Method of Solution.*—The problem investigated is the diffusion of stress in a flat, or slightly cambered, symmetrical wing surface near chordwise gaps in the inter-spar skin and stringers; such gaps occur where the spar flanges alone are fixed, for example, at a wing joint, and at undercarriage and bomb-bay cut-outs.

It is assumed that the front and rear spars are equal in depth, and then, on the basis of Engineering (Simple Beam) Theory, there is no chordwise variation of direct stress across a section (say AA' in Fig. 1) not near a chordwise gap.

*R.A.E. Report No. S.M.E. 3208, received 13th July, 1942. Revised by one of the authors (H.G.H.), May, 1950.

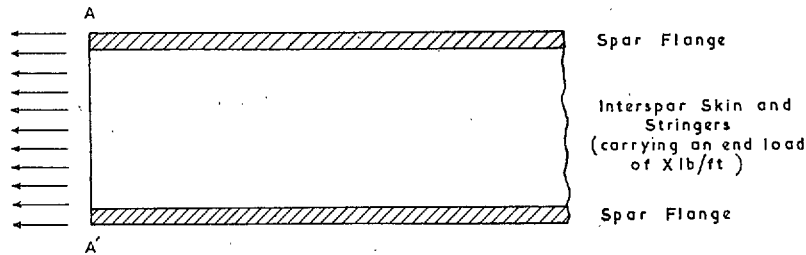


FIG. 1. Distribution of direct stress across section AA' not near a chordwise gap

If now the wing surface is imagined cut between the spars at the section AA', the direct end load originally carried by the inter-spar skin and stringers (as shown in Fig. 1) is now necessarily carried by the spar flanges, and its magnitude is easily calculated in any particular case. The distribution of stress across the section AA' is now as shown in Fig. 2; in practice, the section AA' would have some spanwise stiffening from a rib, and then there would still be some direct end load applied to the inter-spar skin and stringers at the section AA', its magnitude being dependent upon the spanwise bending stiffness of the rib flange but in any event this direct end load would have been greatly reduced by the chordwise cut.

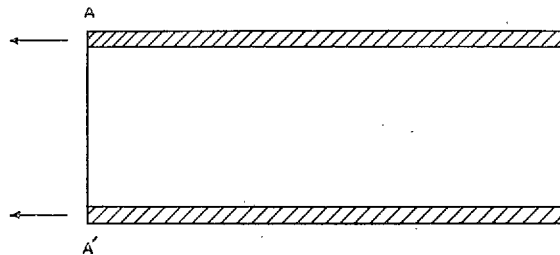


FIG. 2. Distribution of direct stress across section AA' at a chordwise gap

The new stress distribution (Fig. 2) is obtained by the super-position of the original stress distribution (Fig. 1) and that produced by the self-equilibrating system of direct end load applied at the section AA' shown in Fig. 3.

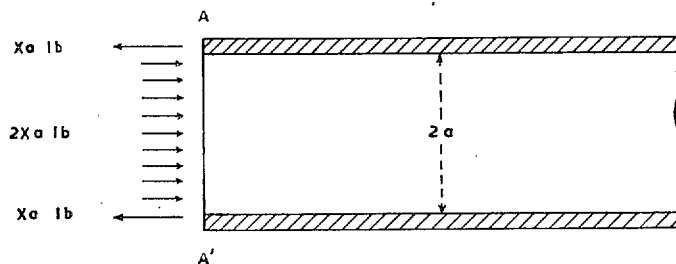


FIG. 3. Self-equilibrating system of direct end load at section AA'

The stress distribution at any section of the wing not near a chordwise gap is calculated with sufficient accuracy on the basis of Engineering Theory.* The stress distribution at a section of the wing near a chordwise gap is therefore calculable if it is calculable for the case shown in Fig. 3. This latter stress distribution is due to a self-equilibrating system of direct end load at the section AA', and therefore, by Saint-Venant's principle, is largely confined to the immediate neighbourhood of this section. It follows that little loss in accuracy will occur if spanwise variations (supposed smooth) in wing structure are neglected. For convenience, the theoretical analysis is

*This is least accurate near the wing root, but even there it will serve to enable a safe estimate to be made of the effect of a chordwise gap.

of the doubly-symmetrical load distribution problem shown in Fig. 4. If the panel (Fig. 4) is long in comparison with its width, then the stress distribution near the section AA' is determined mainly by the applied loads at this section only and little influenced by those at the section CC'. Experimental and theoretical work show that, in general, if $AB/AO > 1.5$, then the panel may be regarded as long in this sense with negligible error.

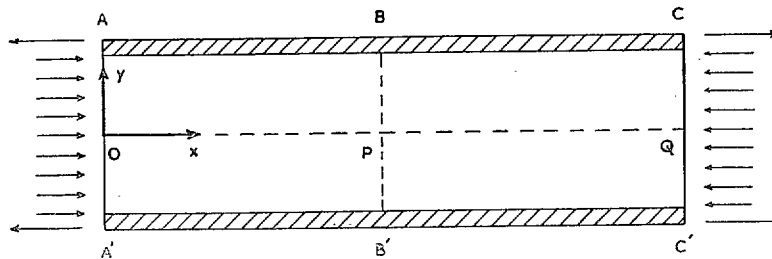


FIG. 4. Doubly-symmetrical panel with self-equilibrating systems of direct end load at sections AA' and CC'

The theoretical analysis of the problem shown in Fig. 4 is set out in the Appendix; it is assumed there that (i) the stringers are adequately represented by a uniform sheet, carrying direct end load only and (ii) the chordwise component of the displacement of the stringer-sheet and skin is negligible in comparison with the spanwise component; the first assumption involves little error if the stringer pitch is small compared with the inter-spar distance, and the second assumption also involves little error because the ratio of chordwise to spanwise stiffness of the rib flanges is usually high. (It may be noted that it is straightforward to extend the theoretical analysis to include the spanwise bending stiffness of the flange of the rib normally present at the section AA'.) As a further simplification it is assumed that the skin thickness, stringer area and stringer pitch are constant; this is closely representative of current practice. The theoretical analysis, although straightforward, does not lead to expressions for the stresses that are capable of rapid computation for the range of cases of practical importance. Further, the analysis predicts an infinite shear stress in the skin at the corners of the panel, and this has no physical reality. For these reasons simple approximate formulae are found for the stresses of most practical importance. The accuracy of the approximate formulae for these stresses is gauged from Figs. 9 to 11 where, for a particular case, these are compared with the accurate formulae for the stresses. The accuracy is sufficient for practical purposes.

3. Notation.

- $2l$ length of panel (*i.e.*, AC in Fig. 4)
- $2a$ width of panel (*i.e.*, AA' in Fig. 4)
- t skin thickness
- t_s stringer-sheet thickness, viz. (total stringer area and effective skin area) \div panel width
- E Young's modulus of flanges, skin and stringers
- F flange area
- G effective shear modulus of skin
- p flange direct stress at gap
- p_x approximate value of flange direct stress at distance x (measured spanwise) from gap (*see* Fig. 4)
- q_x approximate value of skin shear stress at flanges at distance x (measured spanwise) from gap (*see* Fig. 4)
- q_y approximate value of skin shear stress at gap at distance y (measured chordwise) from centre-line between spar flanges (*see* Fig. 4).

Note that in the calculation of t_s allowance is to be made for the capacity of the skin to carry direct stress; of course, on the tension side of the wing the skin is fully effective (assuming that torsional shear stresses have not already caused skin buckling), and on the compression side of the wing the effectiveness of the skin depends on the degree of buckling (*see* Ref. 2). Similar remarks apply to the calculation of G , the effective shear modulus of the skin.

4. *Approximate Formulae for the Stresses.*—Approximate formulae are now given for (i) the direct stress in the flanges (section 4.1) and (ii) the shear stress in the skin at the flanges (section 4.2) and at the chordwise gap (section 4.3). As already stated in section 2, these stresses refer to the problem shown in Fig. 3, and must be added to the stresses (calculated on the basis of Engineering Theory) for the problem shown in Fig. 1 to give the stresses for the problem of the chordwise gap shown in Fig. 2. The error involved in the use of these approximate formulae, in comparison with the accurate formulae, is negligible if the panel is such that

$$(a/l) (Et_s/Gt)^{1/2} < 1.3.$$

4.1. *Direct Stress in the Flanges.*—This is given approximately for the formula

$$p_x/p = e^{-K_1 x/a} \quad (0 \leq x \leq l), \quad \dots \dots \dots (1)$$

where K_1 is found from Fig. 5 after calculation of the non-dimensional parameters F/at_s and $(Et_s/Gt)^{1/2}$. The variation of p_x/p with the non-dimensional parameter $K_1 x/a$ is shown in Fig. 6.

4.2. *Shear Stress in the Skin at the Flanges.*—This is given approximately by the formula

$$q_x/p = - (K_1 F/at) e^{-K_1 x/a} = - (K_1 F/at) p_x/p \quad (0 \leq x \leq l), \quad \dots (2)$$

where K_1 is defined in section 4.1. (Thus there is a simple relation between p_x and q_x .) It is found (see section 5) that this formula can give large values for the skin shear stress at the corners A and A' of the panel (see Fig. 4); in practice, local plastic flow and buckling will afford relief of these stresses, and moreover, the flexibility of the riveted joints between the spar flanges and the skin should be considered in relation to the stress concentration.

4.3. *Shear Stress in the Skin at the Gap.*—This is given approximately by the formula

$$q_y/p = - (K_1 F/at \sinh K_2) \sinh (K_2 y/a) \quad (-a \leq y \leq a), \quad \dots (3)$$

where K_1 is defined in section 4.1, and K_2 is found from Fig. 7 after calculation of the non-dimensional parameters F/at_s and $(a/l) (Et_s/Gt)^{1/2}$. The variation of $-(at \sinh K_2/K_1 F) q_y/p$ with $K_2 y/a$ is shown in Fig. 8. The remarks made at the end of section 4.2 also apply here.

5. *Numerical Example to Illustrate Application to Design.*—A numerical example is now given to illustrate the application to design. As a typical case, consider a panel representing the wing surface between an encasté wing root and a chordwise gap such that:

- $2a$ (inter-spar distance) = 40 in.,
- l (distance between encasté wing root and gap) = 70 in.,
- t (skin thickness) = 0.028 in.,
- t_s (stringer-sheet thickness) = 0.056 in.,
- F (spar flange area) = 1.12 sq. in.,
- $G/E = 0.4$.

Suppose that, if there were no gap, the uniform direct stress is p lb. per sq. in. The total direct end load carried by the interspar skin and stringers is then $40 \times 0.056p = 2.24p$ lb. The additional direct end load carried by each spar flange when there is a gap is $1.12p$ lb.; the additional direct stress is therefore p lb./sq. in.

(i) *Direct stress in the flanges.*—Calculation shows that $(Et_s/Gt)^{1/2} = (0.056/0.4 \times 0.028)^{1/2} = 2.24$ and $F/at_s = 1.12/(20 \times 0.056) = 1$; therefore, from Fig. 5, $2.24K_1 = 2.73$, i.e. $K_1 = 1.22$, and then $K_1/a = 1.22/20 = 0.061$. Now, when $K_1 x/a = 1$, $x = a/K_1 = 20/1.22 = 16.4$, and therefore, in Fig. 6, where the variation of p_x/p is shown, the abscissa scale is $1/16.4$.

(ii) *Shear stress in the skin at the flanges.*—Calculation shows that

$$K_1 F/at = (1.22 \times 1.12)/(20 \times 0.028) = 2.44.$$

Therefore this shear stress is -2.44 times the flange stress (see (i) above).

(iii) *Shear stress in the skin at the gap.*—Calculation shows that

$$(a/l) (Et_s/Gt)^{1/2} = (20/70) \times 2.24 = 0.64;$$

also $F/at_s = 1$, and therefore, from Fig. 7, $K_2 = 2.26$. Now, when $K_2 y/a = 1$,

$$y = a/K_2 = 20/2.26 = 8.9,$$

and therefore, in Fig. 8, where the variation of q_y/p is shown, the abscissa scale is $1/8.9$. Now $\sinh 2.26 = 4.74$, and hence $K_1 F/at \sinh K_2 = 2.44/4.74 = 0.51$; therefore, the ordinates in Fig. 8 are multiplied by 0.51 to give $-q_y/p$.

The stresses found above must be added to the stresses that would be present if there were no gap; as stated previously, these latter stresses are found with sufficient accuracy from Engineering Theory.

6. *Conclusions.*—The numerical example of section 5 shows that the additional shear stress in the skin at a corner can be two to three times the additional flange direct stress there. The example taken is representative of current practice, and the above result therefore shows that some reinforcement of the skin is probably necessary at the corners. However, various factors are likely to reduce the stress concentration if calculations on the present basis predict it to be high; for example, local plastic flow and buckling will afford relief, and, moreover, the flexibility of the riveted joints between the spar flanges and the skin should be considered in relation to the stress concentration.

REFERENCES

<i>No.</i>	<i>Author(s)</i>	<i>Title, etc.</i>
1	D. Williams, R. D. Starkey and R. H. Taylor	Distribution of Stress between Spar Flanges and Stringers for a Wing under Distributed Loading. R. & M. 2098. June, 1939.
2	M. Fine	A Comparison between Plain and Stringer-reinforced Sheet from the Shear-lag Standpoint. R. & M. 2648. October, 1941.

APPENDIX

Mathematical Analysis

Additional notation :

- u component, parallel to Ox, of stringer-sheet and skin displacement,
- σ stringer-sheet and skin direct stress over elements normal to Ox,
- τ skin shear stress,
- u_F flange displacement,
- σ_F flange direct stress,
- $p = (\sigma_F)_{x=0, 2l}$ flange direct stress at panel ends,
- $-\dot{p}_s = (\sigma)_{x=0, 2l}$ (constant) stringer-sheet and skin direct stress at panel ends,
- $k = (Et_s/Gt)^{1/2}$,
- $\alpha = F/at_s, \beta = F/lt, \gamma = \pi ka/2l$,
- $c_n = \cosh n\gamma, s_n = \sinh n\gamma, t_n = \tanh n\gamma$ ($n = 1, 3, \dots$).

This Appendix gives the mathematical analysis of the problem shown in Fig. 4, subject to certain simplifications described in section 2.

If $\partial^2 u / \partial x^2$, for fixed y ($-a \leq y \leq a$), is a continuous function of x in the range ($0 \leq x \leq 2l$) then it may be expanded as a half-range Fourier cosine series* in the range ($0 \leq x \leq 2l$), *i.e.*

$$\frac{\partial^2 u}{\partial x^2} = Y_0(y) + \sum_{n=1}^{\infty} Y_n(y) (n\pi/2l)^2 \cos(n\pi x/2l) \quad (0 \leq x \leq 2l, -a \leq y \leq a), \quad (12)$$

where the $Y_n(y)$'s are continuous functions of y only, and the coefficient $(n\pi/2l)^2$ is introduced for convenience. The stress field is symmetrical about the lines $y = 0$ and $x = l$; hence, firstly

$$Y_n(y) = Y_n(-y) \quad (n = 0, 1, 2, \dots), \quad \dots \quad \dots \quad \dots \quad \dots \quad \dots \quad (13)$$

and secondly $\frac{\partial^2 u(x, y)}{\partial x^2} = \frac{\partial^2 u(2l - x, y)}{\partial x^2}$ which leads to**

$$Y_n(y) \equiv 0 \quad (n = 0, 2, 4, \dots). \quad \dots \quad \dots \quad \dots \quad \dots \quad \dots \quad (14)$$

Therefore,

$$\frac{\partial^2 u}{\partial x^2} = \sum_{n=1, 3, \dots}^{\infty} Y_n(y) (n\pi/2l)^2 \cos(n\pi x/2l) \quad (0 \leq x \leq 2l, -a \leq y \leq a). \quad \dots \quad (15)$$

The integration of equation (15), with use of equations (8) and (10), gives

$$u = - \sum_{n=1, 3, \dots}^{\infty} \{Y_n(y) \cos(n\pi x/2l) - Y_n(a)\} - \alpha p x / E \quad (0 \leq x \leq 2l, -a \leq y \leq a). \quad (16)$$

Substitute equation (16) in equation (4), and carry out the differentiations of the infinite series term-by-term; then

$$\sum_{n=1, 3, \dots}^{\infty} \{(n\pi/2l)^2 Y_n(y) - \frac{1}{k^2} Y_n''(y)\} \cos(n\pi x/2l) = 0 \quad (0 \leq x \leq 2l, -a \leq y \leq a), \quad (17)$$

which leads to**

$$Y_n''(y) - \frac{n^2 \gamma^2}{a^2} Y_n(y) = 0 \quad (n = 1, 3, \dots) \quad (-a \leq y \leq a), \quad \dots \quad \dots \quad (18)$$

From equations (13) and (18)

$$Y_n(y) = A_n \cosh(n\gamma y/a) \quad (n = 1, 3, \dots) \quad (-a \leq y \leq a), \quad \dots \quad \dots \quad (19)$$

where the A_n 's are constants, and therefore equation (16) is

$$u = - \sum_{n=1, 3, \dots}^{\infty} A_n \{\cosh(n\gamma y/a) \cos(n\pi x/2l) - c_n\} - \alpha p x / E \quad (0 \leq x \leq 2l, -a \leq y \leq a). \quad (20)$$

If $d^2 u_F / dx^2$ is a continuous function of x in the range ($0 \leq x \leq 2l$), then it may be expanded as a half-range Fourier cosine series in the range ($0 \leq x \leq 2l$), *i.e.*

$$\frac{d^2 u_F}{dx^2} = A_0' + \sum_{n=1}^{\infty} A_n' (n\pi/2l)^2 \cos(n\pi x/2l) \quad (0 \leq x \leq 2l), \quad \dots \quad \dots \quad (21)$$

where the A_n' 's are constants, and the coefficient $(n\pi/2l)^2$ is introduced for convenience. The stress distribution is symmetrical about the line $x = l$; hence $\frac{d^2 u_F(x)}{dx^2} = \frac{d^2 u_F(2l - x)}{dx^2}$ which leads to (*see** footnote below*)

$$A_n' = 0 \quad (n = 0, 2, 4, \dots). \quad \dots \quad \dots \quad \dots \quad \dots \quad \dots \quad (22)$$

*The relevant properties of Fourier series are given in: Fourier's Series and Integrals, by H. S. Carslaw (London, 1921).

**Multiply the equation by $\cos(n'\pi x/2l)$ ($n' = 0, 1, 2, \dots$) and integrate the infinite series term-by-term with respect to x over the range ($0 \leq x \leq 2l$); finally replace n' by n . For conciseness, when this procedure occurs elsewhere, reference is made to this footnote.

Therefore,

$$\frac{d^2 u_F}{dx^2} = \sum_{n=1,3,\dots}^{\infty} A_n' (n\pi/2l)^2 \cos(n\pi x/2l) \quad (0 \leq x \leq 2l). \quad \dots \quad (23)$$

The integration of equation (23), with use of equations (8) and (10), gives

$$u_F = - \sum_{n=1,3,\dots}^{\infty} A_n' \{ \cos(n\pi x/2l) - 1 \} + px/E \quad (0 \leq x \leq 2l). \quad \dots \quad (24)$$

Substitute equations (20) and (24) in equation (7), and carry out the differentiations of the infinite series term-by-term; then

$$\sum_{n=1,3,\dots}^{\infty} (A_n s_n + A_n' \alpha \gamma n) \cos(n\pi x/2l) \quad (0 \leq x \leq 2l), \quad \dots \quad (25)$$

which leads to (*see** footnote on p. 7*)

$$A_n s_n + A_n' \alpha \gamma n = 0 \quad (n = 1, 3, \dots). \quad \dots \quad (26)$$

From equations (9), (20) and (24),

$$\sum_{n=1,3,\dots}^{\infty} (A_n c_n - A_n') \{ \cos(n\pi x/2l) - 1 \} + (1 + \alpha) px/E = 0 \quad (0 \leq x \leq 2l), \quad \dots \quad (27)$$

which leads to (*see** footnote on p. 7*)

$$A_n c_n - A_n' = 8(1 + \alpha) pl/n^2 \pi^2 E \quad (n = 1, 3, \dots). \quad \dots \quad (28)$$

From equations (26) and (28),

$$\left. \begin{aligned} A_n &= 8\alpha(1 + \alpha) \gamma pl/n (\alpha \gamma n + t_n) c_n \pi^2 E, \\ A_n' &= -8(1 + \alpha) t_n pl/n^2 (\alpha \gamma n + t_n) \pi^2 E, \end{aligned} \right\} (n = 1, 3, \dots), \quad \dots \quad (29)$$

and then equations (20) and (24) are

$$u = - \frac{8\alpha(1 + \alpha) \gamma pl}{\pi^2 E} \sum_{n=1,3,\dots}^{\infty} \{ \cosh(n\gamma y/a) \cos(n\pi x/2l) - c_n \} / n (\alpha \gamma n + t_n) c_n - \alpha px/E \quad (0 \leq x \leq 2l, -a \leq y \leq a), \quad \dots \quad (30)$$

$$u_F = \frac{8(1 + \alpha) pl}{\pi^2 E} \sum_{n=1,3,\dots}^{\infty} t_n \{ \cos(n\pi x/2l) - 1 \} / n^2 (\alpha \gamma n + t_n) + px/E \quad (0 \leq x \leq 2l), \quad \dots \quad (31)$$

respectively.

To prove that equations (30) and (31) represent the solution of the problem, it is necessary to prove that (i) u and u_F given by equations (30) and (31) respectively, satisfy (a) equation (4) ($0 < x < 2l$, $-a < y < a$) and equation (7) ($0 < x < 2l$), (b) the boundary conditions, equation (8) and (c) the displacement compatibility condition, equation (9), and (ii) the solution is unique with the assumption, equation (10). The analysis required is standard, and, for this reason, is omitted.

From equations (30) and (31), with use of equations (2) and (6), the direct stress in the stringer-sheet and skin, the shear stress in the skin and the direct stress in the flanges are given by,

$$\sigma/p = \frac{4}{\pi} \alpha (1 + \alpha) \gamma \sum_{n=1,3,\dots}^{\infty} \frac{\cosh(n\gamma y/a) \sin(n\pi x/2l)}{(\alpha \gamma n + t_n) c_n} - \alpha \quad (0 \leq x \leq 2l, -a \leq y \leq a), \quad (32)$$

$$\tau/p = -2(1 + \alpha) \beta \sum_{n=1,3,\dots}^{\infty} \frac{\sinh(n\gamma y/a) \cos(n\pi x/2l)}{(\alpha \gamma n + t_n) c_n} \quad (0 \leq x \leq 2l, -a \leq y \leq a), \quad (33)$$

$$\sigma_F/p = -\frac{4}{\pi} (1 + \alpha) \sum_{n=1,3,\dots}^{\infty} \frac{t_n \sin(n\pi x/2l)}{n (\alpha \gamma n + t_n)} + 1 \quad (0 \leq x \leq 2l), \quad \dots \quad (34)$$

respectively.

In particular, from equation (33), the shear stresses in the skin at $x = 0, 2l$ and $y = \pm a$ are given by

$$\tau/p = \mp 2(1 + \alpha) \beta \sum_{n=1,3,\dots}^{\infty} \frac{\sinh(n\gamma y/a)}{(\alpha\gamma n + t_n) c_n} \quad (x = 0, 2l; -a \leq y \leq a), \quad (35)$$

$$\tau/p = \mp 2(1 + \alpha) \beta \sum_{n=1,3,\dots}^{\infty} \frac{t_n \cos(n\pi x/2l)}{(\alpha\gamma n + t_n)} \quad (0 \leq x \leq 2l, y = \pm a); \quad (36)$$

respectively.

Note, from equation (33) that $|\tau| \rightarrow \infty$ as $(x \rightarrow 0, 2l$ and $y \rightarrow \pm a)$, that is, the analysis predicts infinite shear stresses at the corners of the panel.

The above analysis involves the term-by-term differentiation of infinite series and this procedure requires justification. The validity of the term-by-term differentiations of infinite series involved in the solution of elastic problems has often not been justified by writers. The present method of overcoming this difficulty (*see* the analysis immediately following equations (12) and (21)) is an indirect one; a direct method is given by S. Goldstein, Proc. Cambridge Phil Soc., 32 (1936) 40 and 33 (1937) 41.

The analysis of the problem, although straightforward, does not lead to expressions for the stresses that are capable of rapid computation for the range of cases of practical importance. Further, the infinite shear stress predicted at the corners of the panel has no physical reality. For these reasons, simple approximate formulae are now derived for the stresses of most practical importance, *viz.* (i) the direct stress in the flanges and (ii) the shear stress in the skin at the flanges and at the panel ends. Attention is confined to the case in which l/a is not small

The forces applied at either end of the panel form a self-equilibrating system, and therefore, from Saint-Venant's principle, the stresses are small when x/a is large. It is reasonable to suppose that there is an exponential decay of stress along the flanges from either end, *i.e.*

$$\sigma_F/p \approx p_x/p = \begin{cases} e^{-K_1 x/a} & (0 \leq x \leq l), \\ e^{-K_1 (2l-x)/a} & (l \leq x \leq 2l), \end{cases} \quad \dots \dots \dots (37)$$

where $K_1 (> 0)$ is a constant determined from the condition that the areas under the curves for σ_F and p_x are equal, *i.e.*

$$\int_0^l (\sigma_F - p_x) dx = 0, \quad \dots \dots \dots (38)$$

which leads to

$$1/K_1 = (l/a) S(\alpha, \gamma), \quad \dots \dots \dots (39)$$

where

$$S(\alpha, \gamma) = \frac{8}{\pi^2} \sum_{n=1,3,\dots}^{\infty} (n\gamma - t_n)/n^2 (n\gamma + t_n/\alpha) \quad \dots \dots \dots (40)$$

after neglect of a term $e^{-K_1 l/a}$ which is small. From physical considerations, K_1 tends to a definite limit as $l/a \rightarrow \infty$; therefore, from equation (39), for sufficiently small γ , $S(\alpha, \gamma)/\gamma$ is sensibly independent of γ . Computation shows that the relation

$$S(\alpha, \gamma) = \gamma S(\alpha, 1) \quad \dots \dots \dots (41)$$

in the range ($\frac{1}{2} \leq \alpha \leq 2$), involves negligible error for $\gamma \leq 1$, and errors not exceeding + 3½ per cent. and + 11 per cent. in the worst case of $\alpha = 2$ for $\gamma = 1\frac{1}{2}$ and 2, respectively. Therefore,

$$K_1 = 2/\pi k S(\alpha, 1) \quad \dots \dots \dots (42)$$

approximately. The function kK_1 is plotted as a function of α ($\frac{1}{2} \leq \alpha \leq 2$) in Fig. 5.

From the equation of equilibrium of the flanges, equation (5) with use of equation (37),

$$(\tau)_{y=\pm a/p} \simeq q_x/p = \left\{ \begin{array}{ll} \mp (F/at) K_1 e^{-K_1 x/a} & (0 \leq x \leq cl), \\ \mp (F/at) K_1 e^{-K_1 (2l-x)/a} & (l \leq x \leq 2l). \end{array} \right\} \dots \dots (43)$$

It is also reasonable to suppose that

$$(\tau)_{x=0,2l/p} \simeq q_x/p = \mp (F/at) K_1 \frac{\sinh (K_2 y/a)}{\sinh K_2} \quad (-a \leq y \leq a), \dots \dots (44)$$

which is consistent with equation (43) ($x = 0, 2l$) when $y = \pm a$, where $K_2 (> 0)$ is a constant determined from the condition that the areas under the curves for $(\tau)_{x=0}$ and q_y are equal, *i.e.*

$$\int_0^a \{(\tau)_{x=0} - q_y\} dy = 0, \dots \dots (45)$$

which leads to

$$\frac{1}{K_2} \tanh (\frac{1}{2}K_2) = \frac{2(1+\alpha)}{\gamma} S(\alpha, \gamma) \sum_{n=1,3,\dots}^{\infty} (1 - 1/c_n)/n(n\alpha\gamma + t_n) \dots \dots (46)$$

The function K_2 is plotted as a function of α ($\frac{1}{2} \leq x \leq 2$) for various values of the parameter ka/l in Fig. 7.

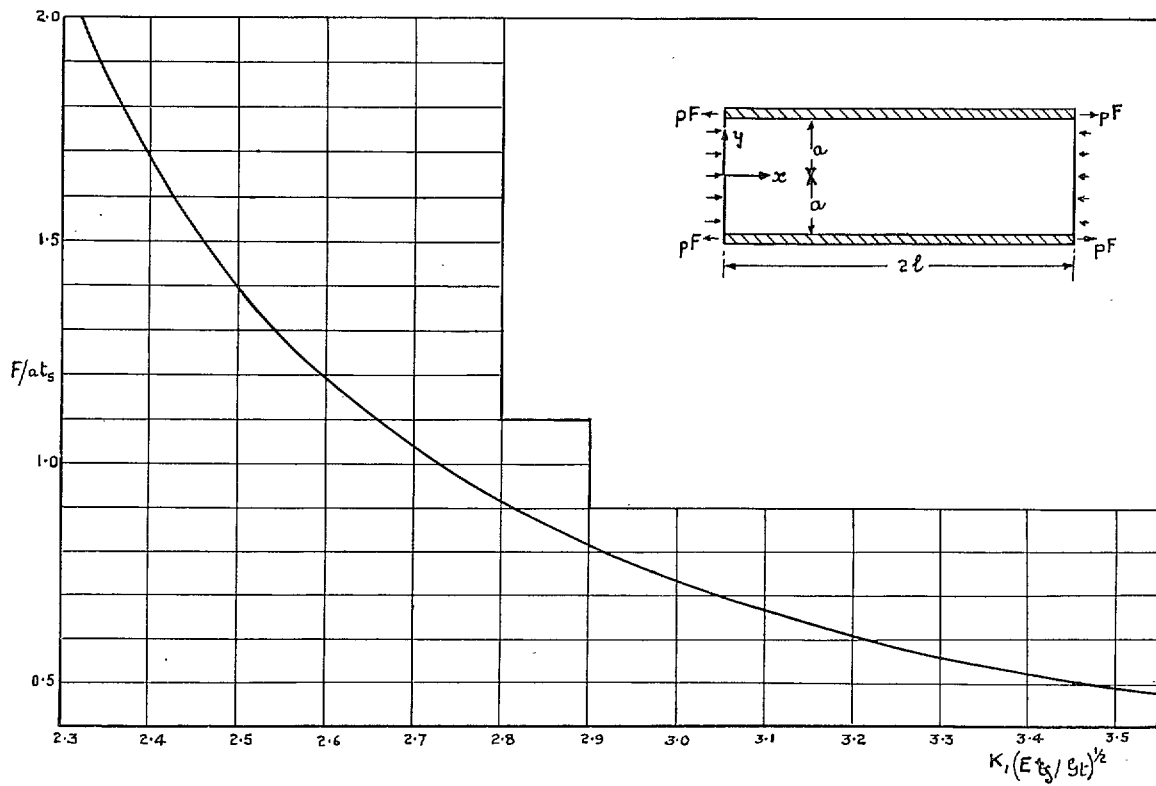


FIG. 5. Graph for determination of K_1

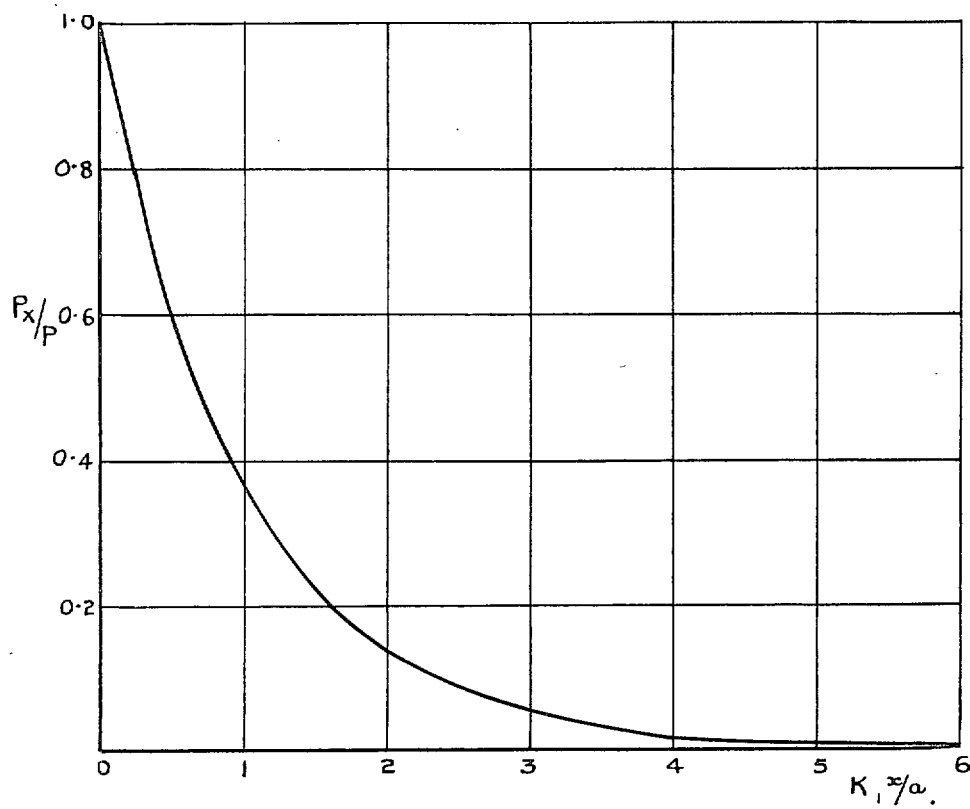


FIG. 6. Variation of flange stress along flange

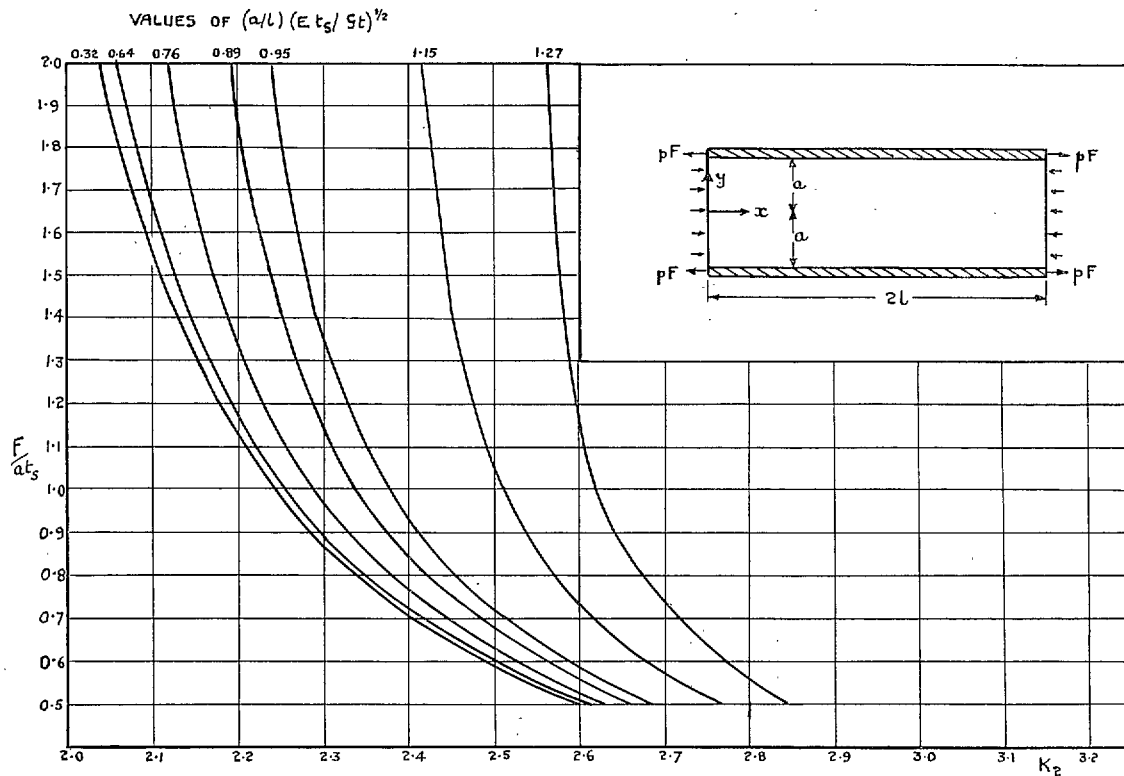


FIG. 7. Graph for determination of K_2

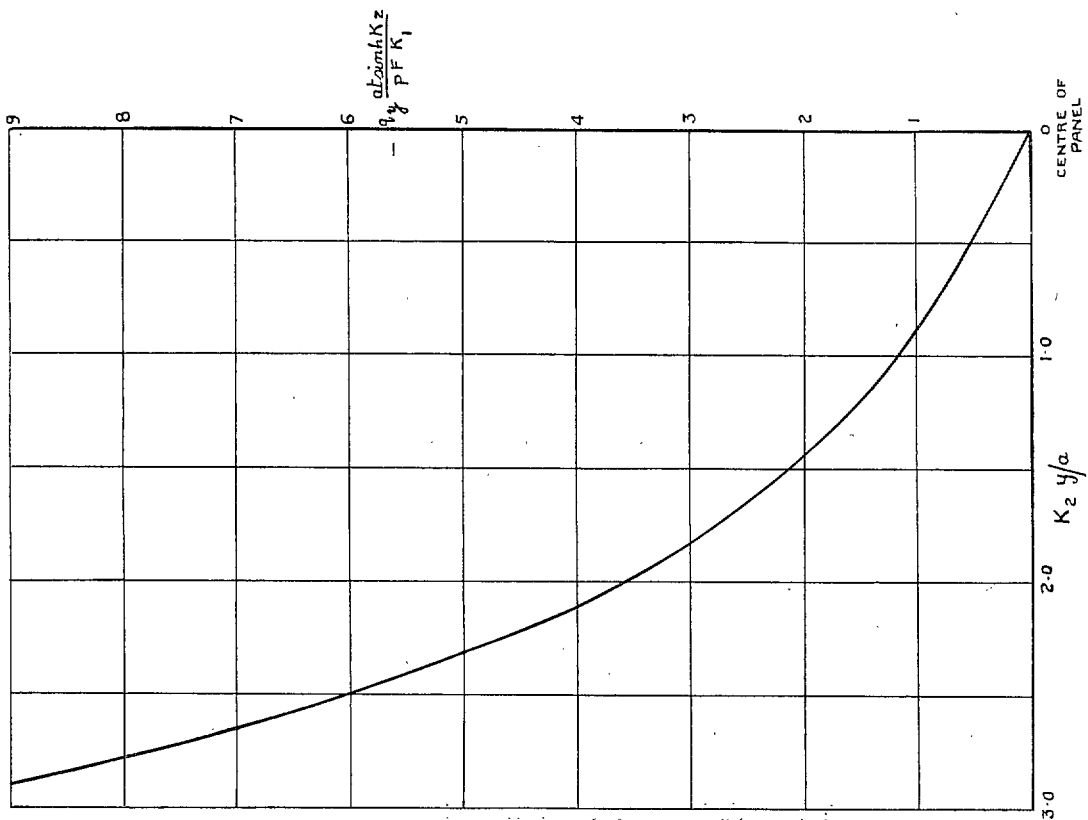


FIG. 8. Variation of shear stress across panel end

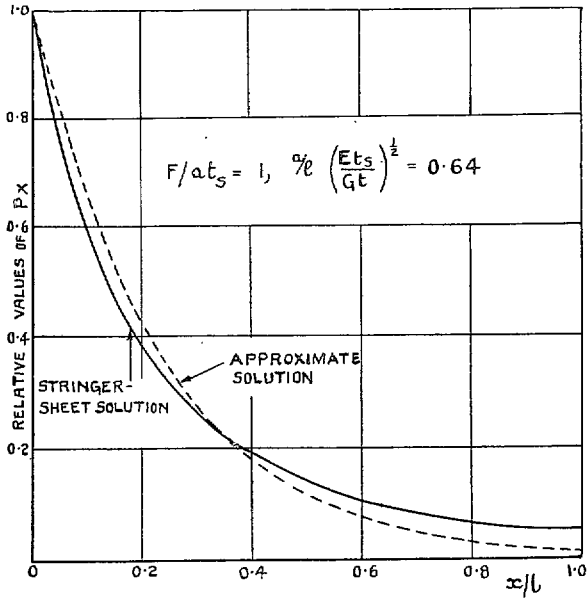


FIG. 9. Comparison of stringer-sheet solution with approximate solution for a typical case: p_x

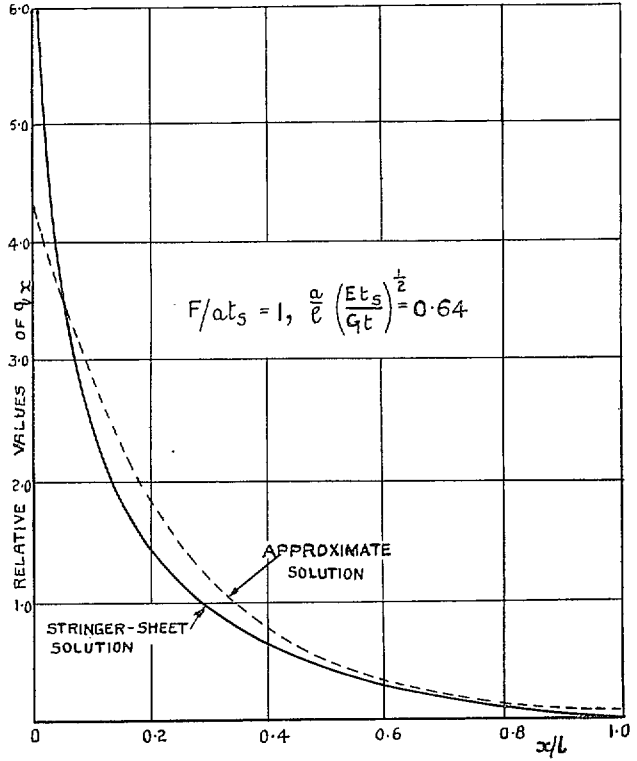


FIG. 10. Comparison of stringer-sheet solution with approximate solution for a typical case: q_x

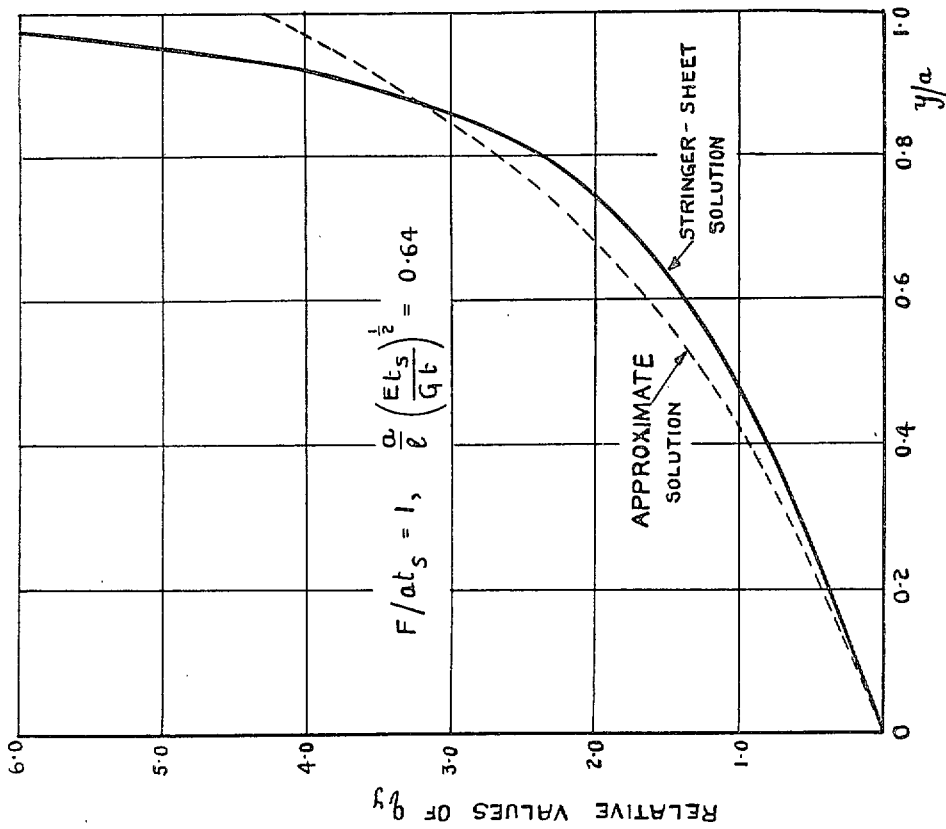


FIG. 11. Comparison of stringer-sheet solution with approximate solution for a typical case: q_y

Publications of the Aeronautical Research Council

ANNUAL TECHNICAL REPORTS OF THE AERONAUTICAL RESEARCH COUNCIL (BOUND VOLUMES)—

- 1934-35 Vol. I. Aerodynamics. *Out of print.*
Vol. II. Seaplanes, Structures, Engines, Materials, etc. 40s. (40s. 8d.)
- 1935-36 Vol. I. Aerodynamics. 30s. (30s. 7d.)
Vol. II. Structures, Flutter, Engines, Seaplanes, etc. 30s. (30s. 7d.)
- 1936 Vol. I. Aerodynamics General, Performance, Airscrews, Flutter and Spinning.
40s. (40s. 9d.)
Vol. II. Stability and Control, Structures, Seaplanes, Engines, etc. 50s. (50s. 10d.)
- 1937 Vol. I. Aerodynamics General, Performance, Airscrews, Flutter and Spinning.
40s. (40s. 10d.)
Vol. II. Stability and Control, Structures, Seaplanes, Engines, etc. 60s. (61s.)
- 1938 Vol. I. Aerodynamics General, Performance, Airscrews. 50s. (51s.)
Vol. II. Stability and Control, Flutter, Structures, Seaplanes, Wind Tunnels,
Materials. 30s. (30s. 9d.)
- 1939 Vol. I. Aerodynamics General, Performance, Airscrews, Engines. 50s. (50s. 11d.)
Vol. II. Stability and Control, Flutter and Vibration, Instruments, Structures,
Seaplanes, etc. 63s. (64s. 2d.)
- 1940 Aero and Hydrodynamics, Aerofoils, Airscrews, Engines, Flutter, Icing, Stability
and Control, Structures, and a miscellaneous section. 50s. (51s.)

*Certain other reports proper to the 1940 volume will subsequently be
included in a separate volume.*

ANNUAL REPORTS OF THE AERONAUTICAL RESEARCH COUNCIL—

1933-34	15. 6d. (15. 8d.)
1934-35	15. 6d. (15. 8d.)
April 1, 1935 to December 31, 1936.	4s. (4s. 4d.)
1937	2s. (2s. 2d.)
1938	15. 6d. (15. 8d.)
1939-48	3s. (3s. 2d.)

INDEX TO ALL REPORTS AND MEMORANDA PUBLISHED IN THE ANNUAL TECHNICAL REPORTS, AND SEPARATELY—

April, 1950 R. & M. No. 2600. 2s. 6d. (2s. 7½d.)

INDEXES TO THE TECHNICAL REPORTS OF THE AERONAUTICAL RESEARCH COUNCIL—

December 1, 1936 — June 30, 1939.	R. & M. No. 1850.	1s. 3d. (1s. 4½d.)
July 1, 1939 — June 30, 1945.	R. & M. No. 1950.	1s. (1s. 1½d.)
July 1, 1945 — June 30, 1946.	R. & M. No. 2050.	1s. (1s. 1½d.)
July 1, 1946 — December 31, 1946.	R. & M. No. 2150.	1s. 3d. (1s. 4½d.)
January 1, 1947 — June 30, 1947.	R. & M. No. 2250.	1s. 3d. (1s. 4½d.)

Prices in brackets include postage.

Obtainable from

HIS MAJESTY'S STATIONERY OFFICE

York House, Kingsway, LONDON, W.C.2 429 Oxford Street, LONDON, W.1
P.O. Box 569, LONDON, S.E.1

13a Castle Street, EDINBURGH, 2 1 St. Andrew's Crescent, CARDIFF
39 King Street, MANCHESTER, 2 Tower Lane, BRISTOL, 1
2 Edmund Street, BIRMINGHAM, 3 80 Chichester Street, BELFAST

or through any bookseller.